Joint strength and interfacial microstructure in silicon nitride/nickel-based Inconel 718 alloy bonding

WOO-CHUN LEE
Center for Materials Evaluation, Korea Research Institute of Standards and Science, P.O. Box 102, Yusong, Taejon 305-600, Republic of Korea

Joining of Inconel 718 alloys to silicon nitrides using Ag–27Cu–3Ti alloys was performed to investigate the microstructural features of interfacial phases and their effect on joint strength. The Si_3N_4/Inconel 718 alloy joints had a low shear strength in the range 70.4–46.1 MPa on average, depending on joining temperature and time. When the joining time was held for 1.26 ks at 1063 K, shear, tension, and four-point bending strength were 70.4, 129.7, and 326.5 MPa on average. The microstructures of the joints typically consisted of six types of phases. They were TiN and Ti_5Si_4 between silicon nitride and filler metal, a copper- and silver-rich phase, island-shaped Ti–Cu phase, a Ti–Cu–Ni alloy layer between filler and base metal, and diffusion of titanium into the Inconel 718 alloys. With increasing joining temperature, the thickness increase of the Ti–Cu–Ni alloy layer was much greater than that of the reaction layer. Thus the diffusion rate of titanium into the base metal was much greater than the reaction rate with silicon nitride. This behaviour of titanium results in the formation of a Ti–Cu–Ni alloy layer in all the joints. The formation of these layers was the cause of the strength degradation of the Si_3N_4/Inconel 718 alloy joints. This fact was supported by the analyses of fracture path after four-point bending strength tests.

1. Introduction

Silicon nitride is used as structural material in advanced heat engines [1], because it exhibits high strength and toughness, good thermal properties, and chemical resistance at elevated temperature. Components for ceramic heat engines [2] currently in use include turbocharger rotors, glow plugs, piston heads, valve sheet heads, and rocker arms. These components consist of mainly ceramic-to-metal joined parts. Ceramic parts are made from silicon nitrides and metallic parts consist of either Ni–Cr–Fe, Fe–Ni–Co, or heat-resistant alloys. A major technique for joining such components is an active-metal brazing method: a direct brazing of metal or ceramic to ceramic using soft metal alloys (e.g. copper, nickel, Ag–Cu, and Au–Ni) with active elements (e.g. titanium, zirconium and hafnium). Joining of heat-resistant alloys to silicon nitrides using this method has been exclusively studied and developed over the past decade. Representative examples are as follows: Si_3N_4/Inconel 600 alloy joining with Ag–27.5Cu–2.0Ti (wt %) [3–5], titanium-coated Si_3N_4/Incoloy 909 alloy and molybdenum joining with Au–18Ni and Ag–28Cu alloys (wt %) [6], Si_3N_4/TA6V alloy joining with Cu–40Ag–5Ti (wt %) [7], titanium-coated Si_3N_4/Incoloy 909 and Inconel 718 alloys joining with Au–5Pa–2Ni alloy (wt %) and the interlayer [4, 8]. Nevertheless, there are a number of problems remaining to be studied, including the method of relieving residual stress generated in the ceramic after joining, the scattering of strength values, etc.

In this work, we joined Ni–Cr–Fe Inconel 718 alloys to silicon nitride ceramics using active metal alloys of the Ag–27Cu–3Ti system. The strength data of this material system have not been reported in detail with the microstructure at the silicon nitride/filler metal and filler metal/Inconel 718 alloy interface. The purpose of this work was to study the microstructural features of the interfacial phases, and the effect of those phases on joint strength.

2. Experimental procedure

2.1. Materials and bonding

Base materials used in these experiments were a pressureless sintered, hot-isostatically-pressed silicon nitride (Ssangyoung Cement, Daejon, Korea; sintering additives $Al_2O_3 + Y_2O_3 < 10\%$, 12.7 mm × 12.7 mm × 4.8 mm and 9.5 mm diameter × 4.6 mm thick), and cold-worked Inconel 718 alloys (Inco Alloys International Inc., Huntingtions, West Virginia). The chemical composition of the Inconel 718 alloy was 56.47Ni–20.56Cr–20.32Fe–1.27Ti–0.5Al–0.04C–0.84bal (at %). Brazing alloys were produced by vacuum-induction melting, multistage annealing, and rolling in the range of 200 μm thick. They were used in the form of thin

0022–2461

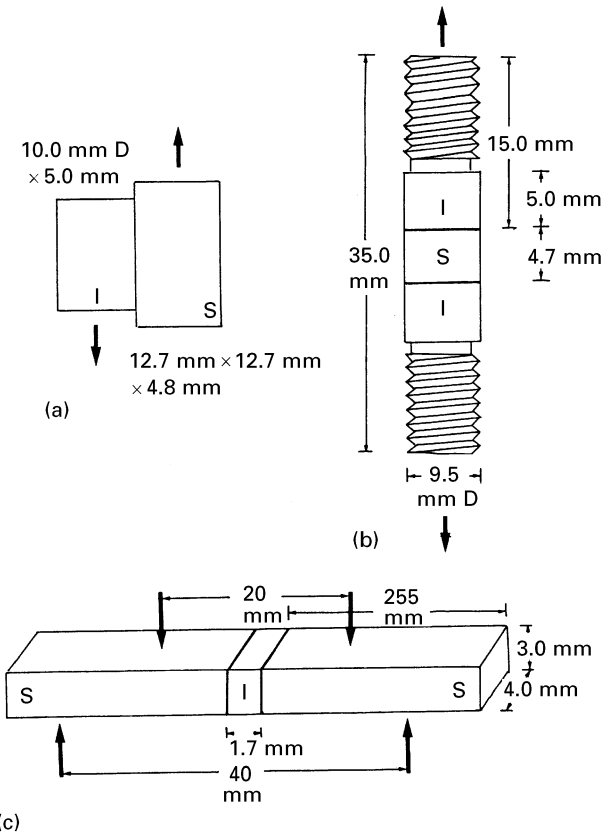

Figue 1 Dimensions of (a) shear, (b) tension, and (c) four-point bending test specimens (S, I, and D stand for silicon nitride, Inconel 718 alloy, and diameter, respectively).

discs (11.0 mm diameter × 0.12–0.15 mm thick). Their chemical compositions were Ag–27.0Cu–3.0Ti (wt %; Ag–37.0Cu–5.5Ti, at %).

Prior to joining, the surface of the silicon nitrides and metals were polished using 15 μm metal-bonded diamond disc and emery paper (no. 1200), cleaned in acetone with ultrasonic vibration, and followed by drying in a hot oven. Bonding was performed in a quartz tube using an infrared heating vacuum furnace ($<2.64\times10^{-3}$ Pa) in the range 1063–1173 K for the time interval of 0.42–2.94 ks. The heating and cooling times were 3.6 and 14.4 ks, respectively.

2.2. Evaluation of strength

The joint strength with joining temperature and time was evaluated by the shear test with an Instron-type tensile test machine using a special jig. The tests were performed three or four times for each condition and the average values were adopted as the shear strengths. The joints showing the highest strength were evaluated by shear, tension, and four-point bending test in order to obtain Weibull data. Fig. 1 shows the dimensions of each test specimen. After joining, the surfaces of tensile and four-point bending specimens were carefully polished using emery paper (no. 1000–2000) and 15 μm metal-bonded diamond disc, respectively. For each test, eight to eleven specimens were measured. The cross-head speed was fixed at 8.33×10^{-5} for all tests.

2.3. Microstructural characterization

The microstructural and chemical analyses of the brazement between silicon nitride and Inconel 718 alloy were carried out using a scanning electron microscope (SEM, AKASHI ISO-DSI30C) equipped with an energy-dispersive X-ray spectrometer (EDX, Rigaku Rotaflex RTP300 RE, 45 kv, 150 mA) and electron probe microanalyser (EPMA, Cameca, SX50). The microstructures of the interfacial reaction products between silicon nitride and filler metal were investigated using an SEM and a cross-sectional transmission electron microscope (TEM, Hitachi H-900 NAR, 300 kV). Chemistries of the reaction products were studied using EDX and a thin-film X-ray diffractometer (XRD, Rigaku Rotaflex RTP300 RE, 45 kV, 150 mA). An XRD analysis was carried out on the reaction products of the thin film which remained on the silicon nitride substrate after mechanically and chemically removing the metallic parts (i.e. Inconel 718 alloy and filler metal) from the Si_3N_4/Inconel 718 alloy joints.

3. Results and discussion

3.1. Shear strength versus joining temperature

Fig. 2 shows the effect of joining temperature on the shear strength of the Si_3N_4/Inconel 718 alloy joints which were brazed for 2.1 ks under 2.64×10^{-3} Pa. From Fig. 2, the shear strength of joints decreased slightly with increasing joining temperature from 1063 K to 1173 K. The joints which were brazed in the temperature range 1063–1173 K had average strength values in the range 61.0–46.1 MPa.

3.2. Shear strength versus joining time

Fig. 3 shows the effect of joining time on the shear strength of the Si_3N_4/Inconel 718 alloy joints. The

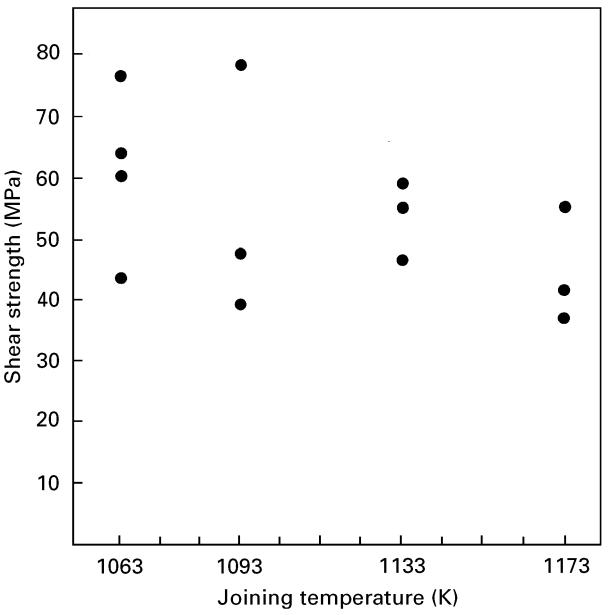

Figure 2 The effect of joining temperature on the shear strength of the Si_3N_4/Inconel 718 alloy joints brazed with 57.5Ag–37.0Cu–5.5Ti (at %) alloy for 2.1 ks under 2.64×10^{-3} Pa.

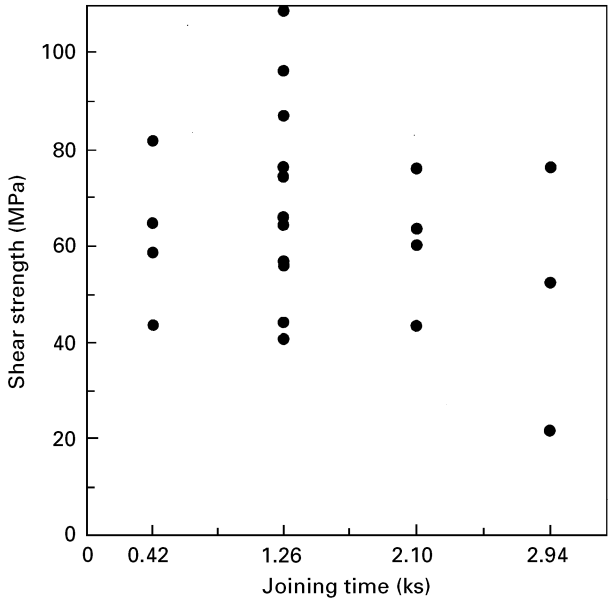

Figure 3 The effect of joining time on the shear strength of the Si_3N_4/Inconel 718 alloy joints brazed with 57.5Ag–37.0Cu–5.5Ti (at %) alloy at 1063 K under 2.64×10^{-3} Pa.

joints were brazed at 1063 K under 2.64×10^{-3} Pa. From Fig. 3, the shear strength of joints increased slightly with the increase of joining time up to 1.26 ks at 1063 K. The joints brazed at the time interval of 0.42–2.94 ks at 1063 K had shear strength values of 70.4–50.4 MPa on average.

From Figs 2 and 3, the joints had the highest strength value of 70.4 MPa on average when the joining time was held for 1.26 ks at 1063 K. Figs 2 and 3 also show that the variation of average shear strength with joining temperature and time was not great. Conclusively, the Si_3N_4/Inconel 718 alloy joints had the low shear strength in the range 70.4–46.1 MPa on average, depending on joining temperature and time.

3.3. Microstructure of the interface and brazement

Fig. 4 shows a backscattered electron image and X-ray maps of each element for a joint brazed at 1063 K for 1.26 ks. Fig. 5 shows SEM microstructures at various brazing temperatures and time. Chemical quantification of the brazements was carried out using EDX and is listed in Table I. As shown in Figs 4 and 5, the joints mainly consist of six types of phases regions. First, the reaction products (A in Fig. 5) formed at the interface between silicon nitride and filler metal. These products were composed of mainly titanium, nitrogen, and silicon, but did not contain nickel which is a main component of Inconel 718 alloy, as shown in Fig. 6b. In addition, Fig. 6a, d show that this product consisted of two or more layers. These layers were TiN and Ti_5Si_4, as shown in Fig. 6e. Consequently, it can be seen that those reaction layers were formed resulting from the redox reaction between silicon nitride and the segregated titanium. As second and third regions, silver-rich phases (B, 89.5Ag–9.7Cu–0.8Ni at %) and copper-rich phases (C, 91.8Cu–2.2Si–4.8Ag–1.2Ni at %) exist in the brazement. Fourth, island-shaped phases (D, 57.3Ni–29.3Ti–6.9Cu–4.5Si–2.0Fe) containing mainly titanium and copper were observed in the filler metal. Ti–Cu island-shaped phases were formed as a result of the reaction between copper and titanium contained in the filler metal. At high temperature, the formation of these phases in the brazement decreased, because the reaction of copper and titanium with base metal became intensive. Fifth, a reaction-product layer (E) was formed between filler and base metal which consisted of 41.0Ti–32.2Cu–25.8Ni–0.78Fe–0.22Cr in atomic percentage. This means that copper and titanium in the filler metal formed a new Ti–Cu–Ni alloy layer through the reaction with nickel after they diffused into the base metal. However, these phases can be mistaken for a liquid form, because these phases did not nearly contain chromium. That is, nickel from the base metal near to the interface can be considered to be selectively reacted with titanium and copper, followed by draining of the remaining chromium into the brazement. If this scenario is correct, the morphology of the liquid phase must be island-shaped. However, these phases formed an interfacial zone in the shape of not islands but bands (or layers), as indicated by E in Fig. 5. Consequently, the Ti–Cu–Ni alloy layer is not liquid but solid phase, i.e. the sixth phase, diffusion of titanium (indicate F) into the base metal was observed. Diffusion of titanium into the base metal increased as the joining temperature and time increased. Consequently, the thickness of the Ti–Cu–Ni alloy layer continued to increase with the joining temperature and time, resulting in the separation from the base metal, as shown in Fig. 7.

3.4. Thickness of interfacial reaction products

Fig. 8 shows the thickness change of the reaction layers at the Si_3N_4/filler metal interface (the "reaction layer") and the Ti–Cu–Ni alloy layers at the filler metal/Inconel 718 alloy interface (the "alloy layer") with the increase of joining temperature at the joining time of 1.26 ks. The thickness of the reaction and alloy layers increased from 2.9 μm to 4.1 μm and from 2.0 μm to 5.4 μm, respectively, as the joining temperature increased from 1063 ks to 1133 ks. With further increase of joining temperature up to 1173 K, the thickness of the reaction layer decreased to 3.3 μm, whereas that of the alloy layer increased rapidly up to 13.8 μm. Thus, at a higher temperature, the growth rate of the Ti–Cu–Ni alloy layer was much greater than that of the reaction product layer. In other words, the diffusion rate of titanium into the base metal was much greater than the reaction rate with silicon nitride. Therefore, if the thickness of the alloy layer increases rapidly, that of the reaction layer rather decreases.

Fig. 9 shows the thickness change of the reaction layer and Ti–Cu–Ni alloy layer with joining time at 1063 K. The thickness of the reaction layer and alloy layers increased from 1.7 μm to 2.1 μm and from 1.0 μm to 2.9 μm, respectively, as the joining time at 1063 K increased from 0.24 ks to 2.10 ks. With further

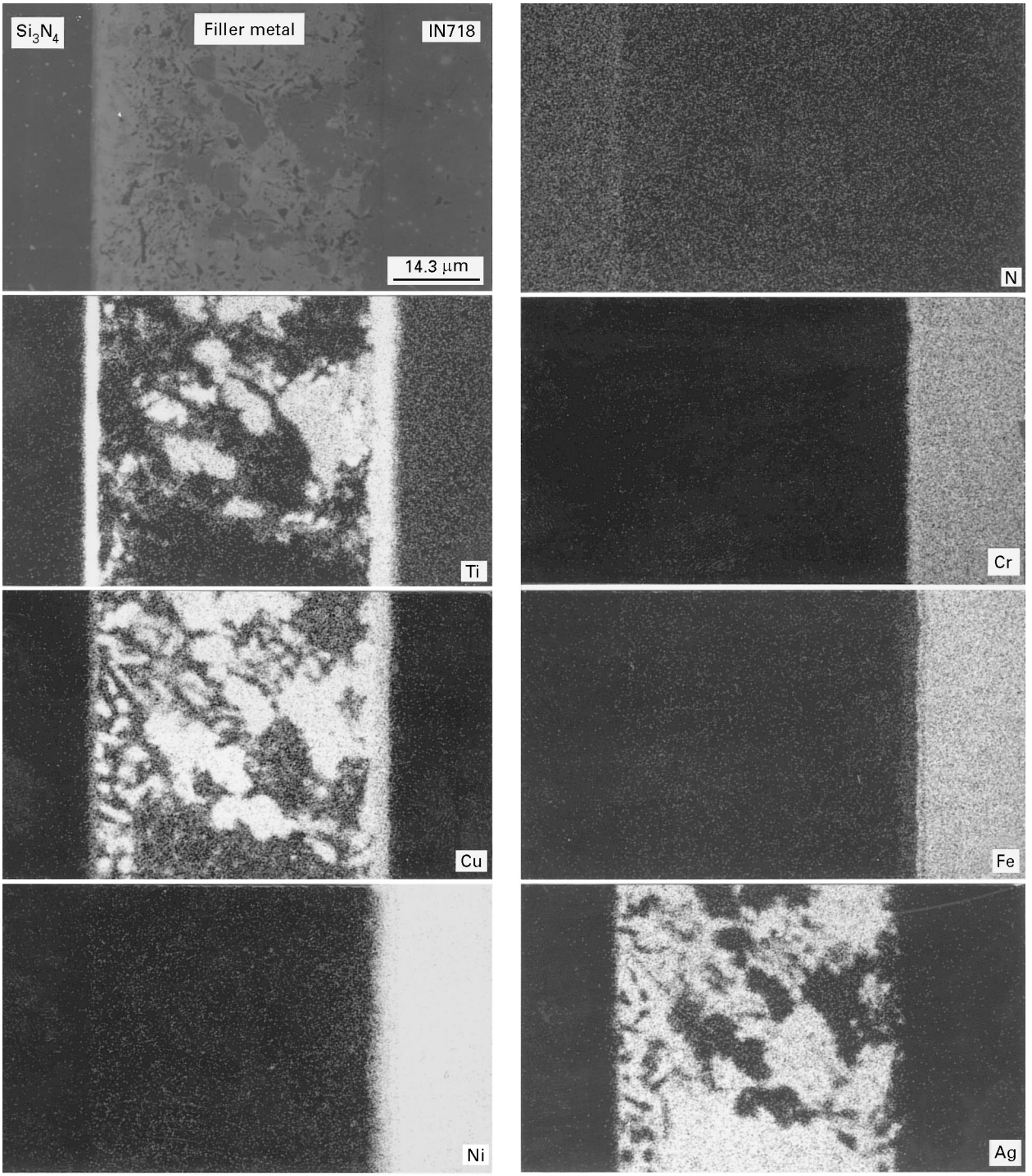

Figure 4 An SEM image and X-ray maps of elements for the brazement of joint brazed with 57.5Ag–37.0Cu–5.5Ti (at %) alloy at 1063 K for 1.26 ks.

increase of joining time up to 2.94 ks, the thickness of the reaction layer decreased slightly to 2.6 μm, whereas that of the alloy layer increased slightly up to 2.3 μm.

From Figs 8 and 9, the effect of joining temperature on the thickness change of the two layers, i.e. alloy layers, was much greater than the joining time. However, despite the thickness change of those layers with the joining temperature and time, Si_3N_4/Inconel 718 alloy joints had low shear-strength values in the range 46.1–70.4 MPa. These results are quite different from those of Si_3N_4/Inconel 600 alloy joints studied previously [9]. The Si_3N_4/Inconel 600 alloy joints at 1063 K for 1.26 ks had higher shear strength (average 160 MPa) than the Si_3N_4/Inconel 718 alloy joints (70.4 MPa). The strength change of joints with joining temperature and time was also very great. In addition, island-shaped Ti–Ni phases existed in the brazement, rather than the formation of Ti–Cu–Ni alloy layers at the filler metal/Inconel 600 alloy interface. Conclusively, Ti–Cu–Ni alloy layers are necessarily formed in the joining of Inconel 718 alloys to silicon nitrides, resulting in the strength degradation of Si_3N_4/Inconel 718 alloy joints throughout all joining conditions.

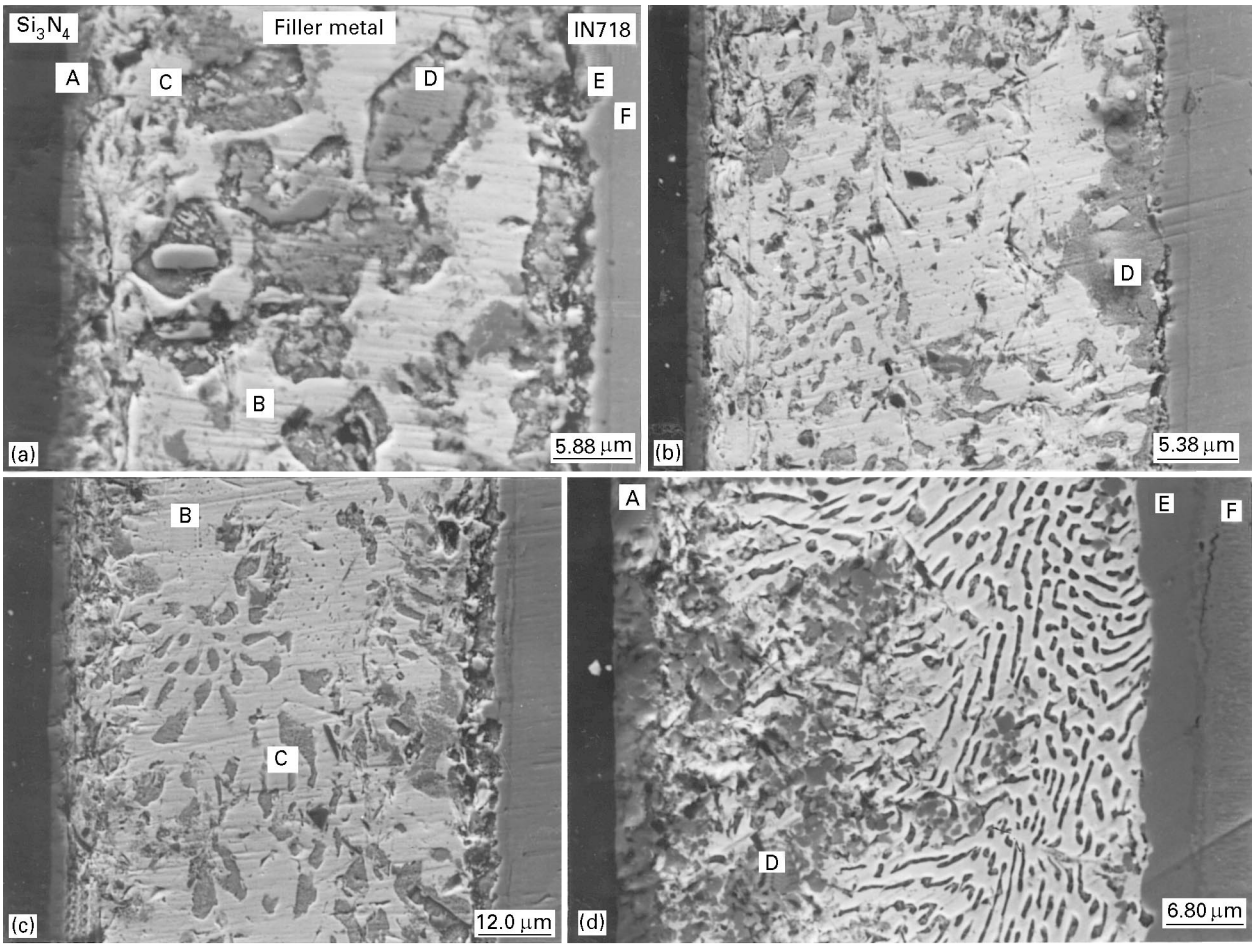

Figure 5 Backscattered electron images for the brazement of joint brazed with 57.5Ag–37.0Cu–5.5Ti (at %) alloy at 1063 K for (a) 0.42 ks, (b) 2.10 ks and (c) 2.94 ks, and (d) at 1133 K for 2.10 ks.

TABLE I EDX semiquantitative analyses (at %) of phases identified in Fig. 5

Phase	Ti	Ni	Cr	Fe	Si	Cu	Ag	Phase
B	–	0.8	–	–	–	9.7	89.5	Ag–rich
C	2.2	1.2	–	–		91.8	4.8	Cu–rich
D	57.3	6.9	–	2.0	4.5	29.3	–	Ti–Cu
E	41.0	25.8	0.22	0.78	–	32.2	–	Ti–Cu–Ni
F	15.0	40.6	29.9	14.5	–	–	–	Base

However, the joints brazed at 1063 K, 1.26 ks had the highest shear strength of 70.4 MPa on average. The reaction layer and alloy layer of this joint were 2.2 and 1.8 μm thick, respectively.

3.5. Weibull distribution of high-strength joints

Fig. 10 and Table II give the Weibull plot and data of shear, tension, and four-point bending strength for the Si_3N_4/Inconel 718 alloy joints which were brazed at 1063 K for 1.26 ks. From Fig. 10 and Table II, average strength values of shear, tension, and four-point bending are seen to be 70.4, 129.7, and 326.5 MPa, respectively. Therefore, the strength ratio was 1 : 1.84 : 4.64 in the order of shear, tension, and four-point bending. Weibull moduli of shear, tension, and four-point bending strength data were 3.60, 3.89, and 9.51, respectively. The Weibull modulus of the four-point bending data was higher than that of shear and tension. Thus the four-point bending test shows lower strength scattering than the shear and tension test.

3.6. Analyses of the fracture path

Fig. 11 shows schematic diagrams of the fracture path after strength tests to obtain Weibull data for the joint brazed at 1063 K for 1.26 ks. From Fig. 11a, the fracture path observed after the shear tests shows that a crack propagated from the perimeter [10] of the bond interface into the inside of silicon nitride. In addition, all of the crack inside of silicon nitride was propagated in a vertical direction to the bond interface. Fig. 11b shows that fracture after the tension test occurred either in the silicon nitride or by varying the path along the bond interface and inside the silicon nitride. In case of tension tests, two types of fracture paths were observed regardless of the strength values. After four-point bending tests, shown in Fig. 11c, fracture occurred either at the filler metal/base metal interface or by varying paths into the bond interface and silicon nitride near to the interface. The cracking at the filler metal/base metal interface indicates that the Ti–Cu–Ni alloy layer at the interface was a path for the fracture. However, four types of

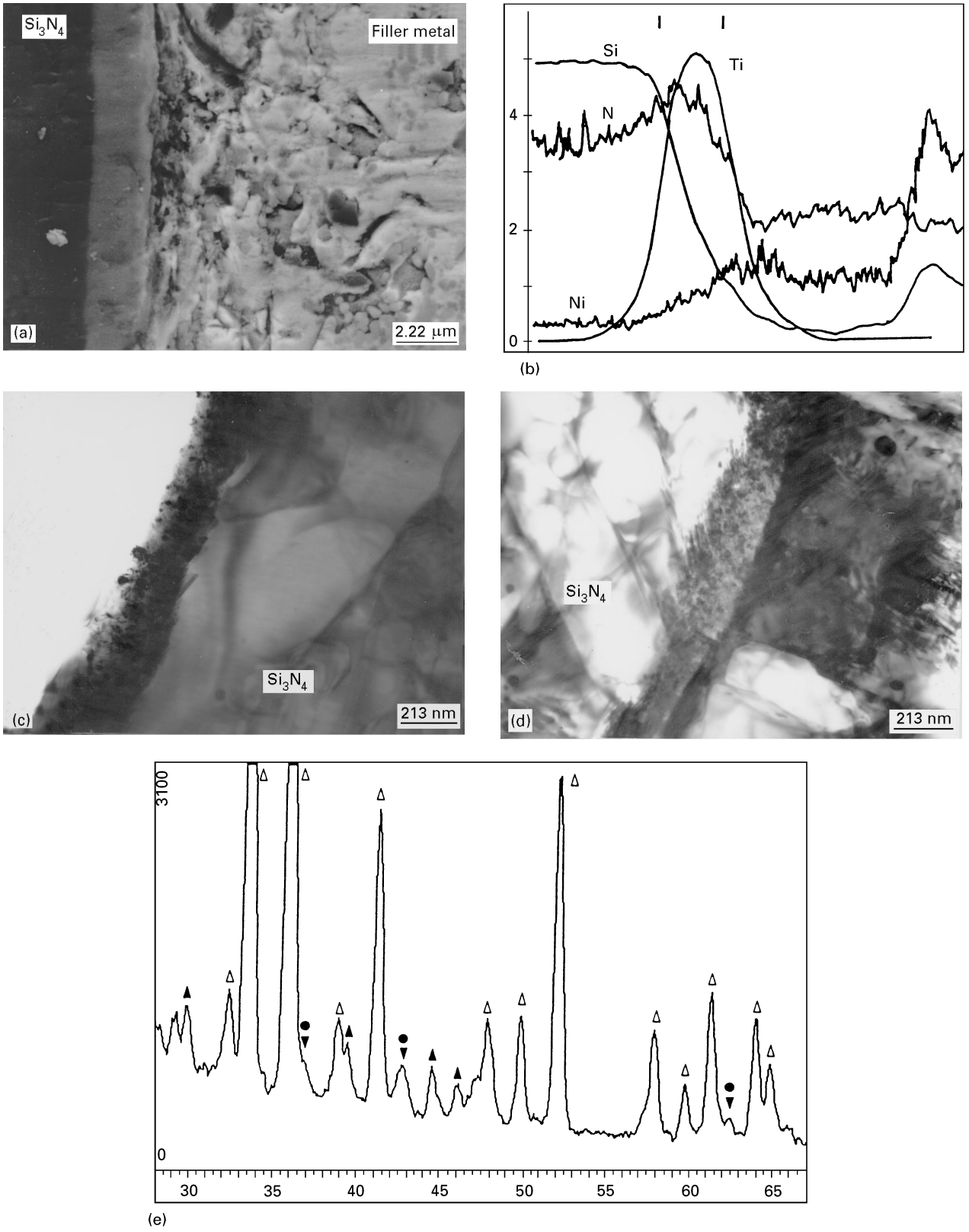

Figure 6 (a) A backscattered electron image, (b) EPMA spectra and (c, d) transmission electron micrographs, and (e) an XRD spectrum of the reaction products between silicon nitride and filler metal for the joints brazed with 57.5Ag–37.0Cu–5.5Ti (at %) alloy at 1063 K for 1.26 ks; (△) β-Si_3N_4, (▲) $Si_2Al_3O_7N$, (▼) TiN, (●) Ti_5Si_4.

fracture paths were also observed regardless of the strength values.

The above results indicate that the fracture path varied depending on the strength test methods. This is because the stress distribution generated in the test piece differed in the different strength test methods.

4. Conclusion

Joint strength (in shear) and microstructures of Si_3N_4/Inconel 718 alloy with joining temperature and time were investigated in order to ascertain the microstructural features of interfacial phases, their effect on joint strength, and Weibull data with strength test methods:

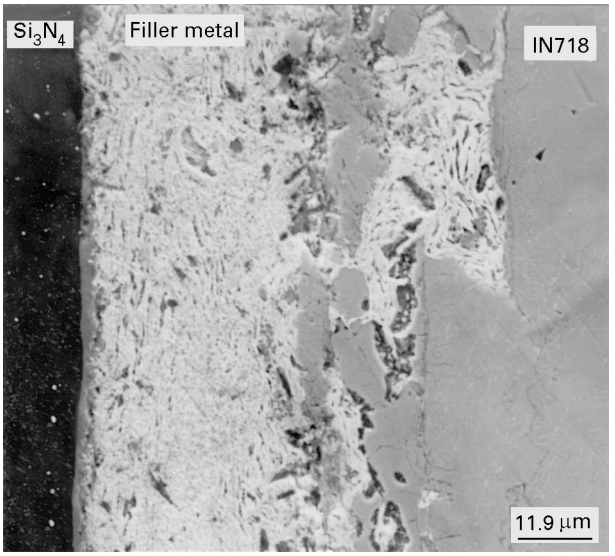

Figure 7 A backscattered electron image of the joint brazed with 57.5Ag–37.0Cu–5.5Ti (at %) alloy at 1173 K for 7.2 ks.

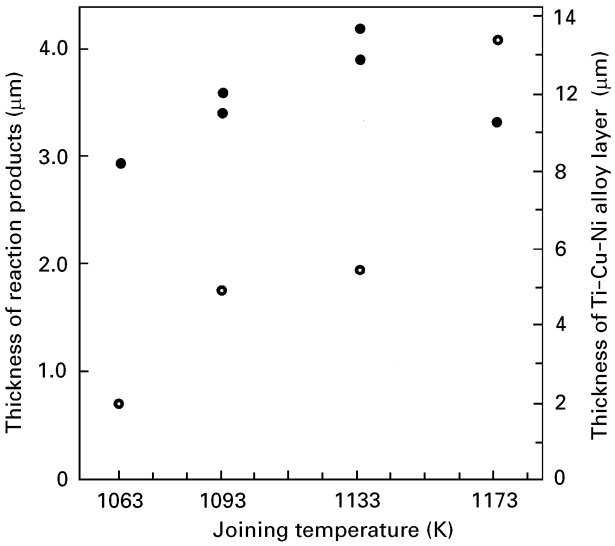

Figure 8 The effect of joining temperature on the thickness of reaction product layers (●) at the Si_3N_4/filler metal interface and Ti–Cu–Ni alloy layer (○) at the filler metal/Inconel 718 alloy interface (joining time 0.42 ks).

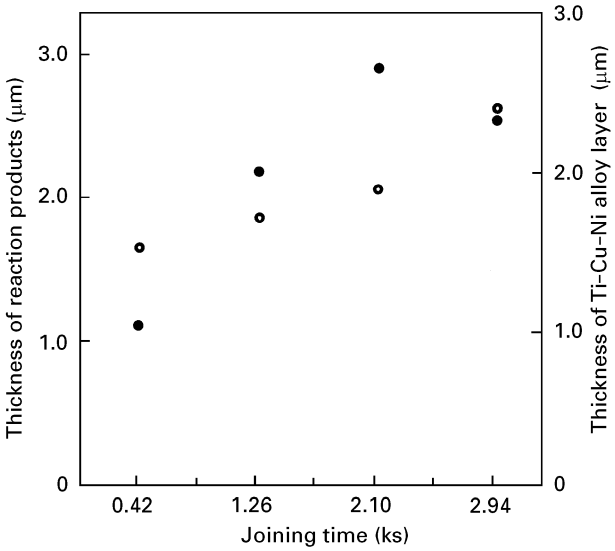

Figure 9 The effect of joining time on the thickness of reaction product layers (○) at the Si_3N_4/filler metal interface and Ti–Cu–Ni alloy layer (●) at the filler metal/Inconel 718 alloy interface (joining temperature 1063 K).

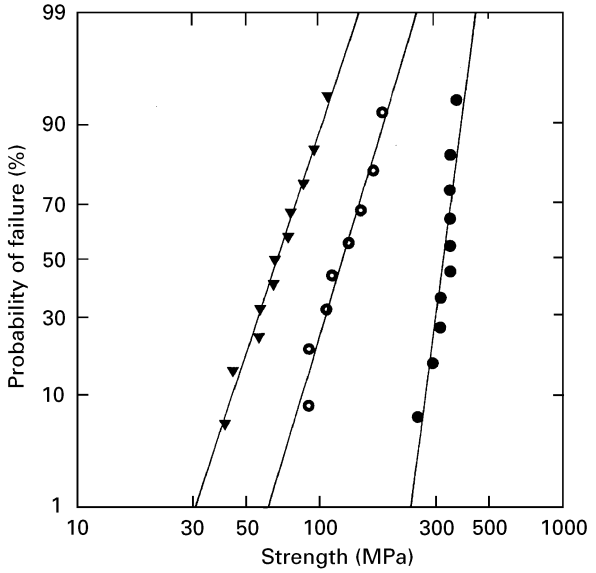

Figure 10 Weibull plot of (▼) shear, (○) tension, and (●) four-point bending strength data for the Si_3N_4/Inconel 718 alloy joints brazed with 57.5Ag–37.0Cu–5.5Ti (at %) alloy at 1063 K for 1.26 ks.

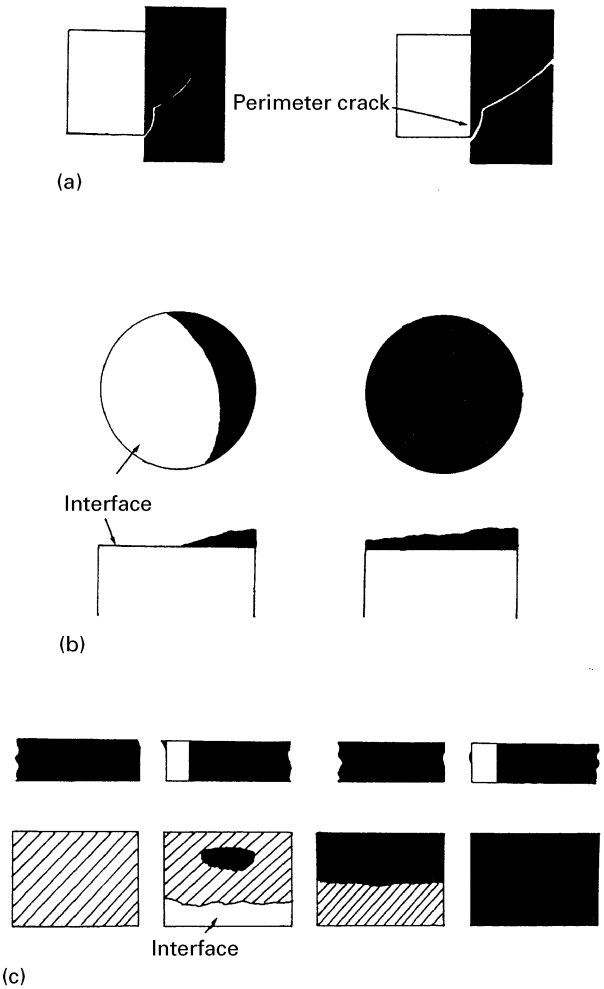

Figure 11 Schematic diagrams of the fracture path observed after (a) shear (side view), (b) tension (top view and side view) and (c) four-point bending tests (top view and side view) for the joints brazed at 1063 K for 1.26 ks (white region, Inconel 718 alloy; black region, silicon nitride; lined area, interface between filler metal and Inconel 718 alloy).

TABLE II Weibull data of shear, tension, and four-point bending strengths for the Si_3N_4/Inconel 718 alloy joint brazed at 1063 K for 1.26 ks

Test method	Average strength (MPa)	Maximum strength (MPa)	Minimum strength (MPa)	Weibull modulus, m	Scale parameter, ξ	Standard deviation (MPa)	Number of tests
Shear	70.4	109.3	40.9	3.60	78.2	21.2	11
Tension	129.7	183.1	90.9	3.89	143.4	34.9	8
Four-point bending	326.5	367.9	251.9	9.51	343.1	34.8	10

shear, tension, and four-point bending. After strength tests, fracture paths were also investigated.

The joint strength decreased slightly with increasing joining temperature and time. However, the Si_3N_4/Inconel 718 alloy joints had a low shear strength in the range 46.1–70.4 MPa on average. When the joining time was held for 1.26 ks at 1063 K, the average strength values of shear, tension, and four-point bending tests were 70.4, 129.7, and 326.5 MPa, respectively. The strength ratio was 1 : 1.84 : 4.64, and the Weibull moduli were 3.60, 3.89, and 9.51, respectively, in the order of shear, tension, and four-point bending. The four-point bending test had lower strength scattering than shear and tension.

The microstructures of joints typically consisted of six types of phases. They were TiN and Ti_5Si_4 between silicon nitride and filler metal, copper- and silver-rich phases, island-shaped Ti–Cu phases, a Ti–Cu–Ni alloy layer between filler and base metal, and diffusion of titanium into the Inconel 718 alloys. The reaction between silicon nitride and filler metal resulted from the redox reaction between silicon nitride and the segregated titanium. On the other hand, Ti–Cu–Ni alloy layers were solid phase which formed through the reaction with nickel from the base metal after copper and titanium in the filler metal diffused into the base metal. With increasing joining temperature, the growth rate of the Ti–Cu–Ni alloy layer was much greater than that of the reaction product layer. In other words, the diffusion rate of titanium into the base metal was much greater than the reaction rate with silicon nitride at the high temperature. This behaviour of titanium results in the formation of a Ti–Cu–Ni alloy layer in all the joints. The formation of these layers between filler metals and Inconel 718 alloys was the cause of the strength degradation of Si_3N_4/Inconel 718 alloy joints. This was identified by analyses of fracture paths after four-point bending strength tests.

References

1. D. S. LARSEN, J. W. ADAMS, L. R. JOHNSON, A. P. S. TEOTIA and L. G. HILL, "Ceramic Materials For Advanced Heat Engines" (Noyes, Park Ridge, NJ, 1985).
2. K. SUGANUMA, in "Joining", edited by R. E. Loehman, in "Engineered Materials Handbook: Ceramics and Glasses", edited by S. J. Shneider (ASM International, The Materials Information Society, Materials Park, OH, 1991) p. 523.
3. S. C. HSU, E. M. DUNN, K. OSTREICHER and T. EMMA, in Proceedings of the International Forum on Structural Ceramics Joining, edited by R. E. Loehman, S. M. Johnson and A. J. Moorhead (American Ceramic Society, Westerville, OH, 1987) p. 1667.
4. J. H. SELVERIAN and S. KANG, *Am. Ceram. Soc. Bull.* **71** (1992) 1551.
5. J. H. CHEN, G. Z. WANG, K. NOGI, M. KAMAI, N. SATO and N. IWAMOTO, *J. Mater. Sci.* **28** (1993) 2933.
6. S. KANG, E. M. DUNN, J. H. SELVERIAN and H. J. KIM, *Ceram. Bull.* **68** (1989) 1608.
7. C. PEYTOUR, F. BABIER and A. REVCOLEVSCHI, *J. Mater. Res.* **5** (1990) 127.
8. J. H. SELVERIAN, D. O'NEIL and S. KANG, *Am. Ceram. Soc. Bull.* **71** (1992) 1403.
9. W.-C. LEE, (1995) unpublished work.
10. A. BARTLETT and A. G. EVANS, *Acta Metall. Mater.* **39** (1991) 1579.

Received 6 March 1995
and accepted 13 June 1996